LANGMUIR

Article pubs.acs.org/Langmuir

Extraction of Au(III) by Microbially Reduced Metal-Organic **Frameworks**

Sarah K. Springthorpe and Benjamin K. Keitz*



Cite This: Langmuir 2021, 37, 9078-9088



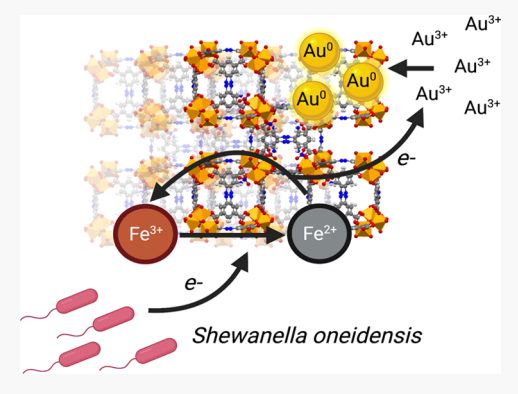
ACCESS I

III Metrics & More



Supporting Information

ABSTRACT: Gold is a critical resource in the jewelry and electronics industries and is facing increased consumer demand. Accordingly, methods for its extraction from waste effluents and environmental water sources have been sought to supplement existing mining infrastructure. Redox-mediated treatments, such as Fe(II)-based platforms, offer promise for precipitating soluble Au(III). We hypothesized that microbial generation of Fe(II) in the presence of sorbent metal-organic frameworks could capitalize on the advantages of both biologicaland chemical-driven extraction approaches. Toward this aim, we tested Au(III) removal by Shewanella oneidensis cultured with Fe(III)-based materials (ferrihydrite, Fe-BTC, MIL-100, or MIL-127). Across all tested materials, S. oneidensis generated the highest levels of redox-active Fe(II) (1.99 \pm 0.27 mM) when cultured with MIL-127 as a respiratory substrate in a bicarbonate-buffered medium. This translated into superior Au(III) removal performance in terms of



both removal rate and capacity ($k = 2.55 \pm 0.60 \text{ h}^{-1}$; $Q = 183 \text{ mg g}^{-1}$). Unlike other materials tested, MIL-127 also maintained cell viability following repeated Au(III) challenges, enabling the regeneration of Fe(II) in the framework. Together, these effects facilitated the treatment of multiple cycles of Au(III) by S. oneidensis-reduced MIL-127. Overall, this work demonstrates that microbial generation of Fe(II) can facilitate the removal of Au(III), augmenting purely adsorptive platforms. Given the biological and chemical modularity of our system, our results suggest that future optimizations to microbial Fe(II) generation may offer promise for improving Au(III) extraction processes.

■ INTRODUCTION

Gold is a precious metal that features resistance to corrosion and high electrical conductivity. As such, it is a crucial component in many electronic devices, and the electronics industry was the second highest consumer of Au in the United States in 2019, following the jewelry industry. The burgeoning demand for electronics combined with their decreased lifetimes puts a strain on this resource's availability, even in light of a growing number of substitutions for the metal in many applications.3 Consequently, there is a significant push to supplement traditional gold mining with recycling from secondary sources, such as electronic waste (e-waste), wastewater effluent, seawater, and freshwater sources where it is found in the parts-per-trillion-parts-per-billion range.4

Traditional methods for Au extraction from alternative sources frequently suffer from production of toxic byproducts, high cost, and incomplete recovery. 9-13 However, adsorptionbased strategies are an emerging alternative that allow for the treatment of larger volumes while limiting both costs and production of byproducts.¹⁴ Several adsorbents have been explored for Au capture, such as activated carbon, ¹⁵ anion-exchange resins, ¹⁶ biomass, ¹⁷ and metal-organic frameworks. ¹⁸ In particular, metal-organic frameworks provide a uniquely tunable platform for Au adsorption. These materials, which are composed of metal ions coordinated to organic

ligands, often exhibit high crystallinity, large surface areas, ordered pore structure, and tunable functional groups, making them promising candidates for extraction platforms with high adsorption capacities. 19,20 Additionally, some metal—organic frameworks contain redox-active metal nodes, allowing them to capture metals through multiple chemical and physical mechanisms. 21-25 For example, it was observed that Au capacities were improved between 4- and 6.8-fold for an Fe(III)-based framework, Fe-BTC, doped with a polymer that reduced the metal centers to Fe(II).2

Despite their generally larger adsorption capacities, metalorganic frameworks generally require a chemical regeneration step for continued Au extraction. For example, redox-active frameworks require isolation and subsequent treatment by a reductant to reduce active components. 23 This can lead to a loss of material every time the adsorbent must be regenerated, resulting in a decrease in performance. An alternative to

Received: April 30, 2021 Revised: July 9, 2021 Published: July 22, 2021





chemical regeneration is to use biological agents as a reductant, with bacteria capable of extracellular electron transfer (EET) being well-poised for this application. These bacteria, which include the Shewanella and Geobacter genera, are capable of transferring electrons onto extracellular substrates under anaerobic conditions. 26 A particular species of the Shewanella genus, Shewanella oneidensis MR-1, has been extensively used as a model for biogenic reduction of insoluble minerals (e.g., iron and manganese oxides) and has been applied for bioremediation. 27,28 We have previously demonstrated that the substrate space for S. oneidensis EET can also include ironbased metal-organic frameworks. When grown on metalorganic frameworks, S. oneidensis showed high efficacy for the remediation of Cr(VI) over multiple cycles, due in large part to the regeneration of Fe(II) by microbial EET. 22 Building on this work, we hypothesized that the use of microbially reduced frameworks could be extended to Au extraction with improved adsorption performance relative to that of the unreduced material or microbes alone.

In this work, we examined the efficacy of microbially reduced metal-organic frameworks for the extraction of Au(III) from solutions. The iron-based frameworks Fe-BTC (BTC = 1,3,5-benzenetricarboxylate), $Fe_3O(BTC)_2(OH)$. nH_2O (MIL-100), and $Fe_3O(H_4TazBz)_{1.5}(H_2O)_3 \cdot nH_2O$ (MIL-127, H_4 TazBz = 3,3′,5,5′-azobenzenetetracarboxylic acid) were reduced by the bacterium S. oneidensis MR-1 to generate Fe(II) prior to challenges of Au(III). These frameworks were chosen as substrates as they are waterstable^{29,30} and contain a well-known Shewanella electron acceptor, Fe(III).31 Previously, we observed that both MIL-100 and Fe-BTC can be used as a respiratory substrate for S. oneidensis MR-1,²² but this had not been tested for MIL-127, which exhibits biocompatibility.³² We demonstrate that S. oneidensis MR-1 can reduce MIL-127 and that this microbially reduced framework can extract Au(III). Cultures of S. oneidensis and MIL-127 featured significantly higher removal of Au(III) than unreduced MIL-127, which we attribute to the microbial generation of redox-active Fe(II). Together, the redox-active properties of MIL-127 paired with the Fe(II) generation power of S. oneidensis enabled an improved Au(III) performance of this framework when compared to that of MIL-100, Fe-BTC, and ferrihydrite (Fh). Finally, we show that S. oneidensis-reduced MIL-127 can undergo successive cycles of Au(III) addition while maintaining Fe(II) regeneration. Overall, our results demonstrate that S. oneidensis-mediated Fe(II) generation with metal-organic frameworks can be leveraged for precious metal recovery and that tuning microbe-material interactions is critical to optimizing the system performance.

MATERIALS AND METHODS

Synthesis of H₄TazBz. H₄TazBz was synthesized by first dissolving 5-nitroisophthalic acid (19 g, 90 mmol) in 250 mL of H₂O and then slowly adding NaOH (50 g, 1.3 mol). The solution was heated at 55 °C until a pink slurry formed. A 150 mL aqueous solution of dextrose (100 g, 0.56 mol) was added slowly to the slurry, forming a brown solution. The solution was removed from heat and stirred overnight under ambient conditions. The resulting mixture was placed in an ice bath prior to filtration. The filtrate was re-dissolved in 200 mL of H₂O, and the solution was acidified to pH = 1 using 12 M HCl. An orange precipitate resulted, which was recovered through filtration, washed with ethanol, and dried at 70 °C (9.66 g; 60% yield). The ligand's structure was verified by ¹H NMR spectra, which matched previous literature reports. Additional character

ization was obtained via liquid chromatography-mass spectrometry (LC-MS) using an Agilent 6530 accurate mass Q-TOF LC/MS apparatus.

Synthesis of Metal-Organic Frameworks and Fh. MIL-127 was synthesized by adding FeCl₃·6H₂O (17.2 g, 63.5 mmol) and H₄TazBz (11.1 g, 31 mmol) to 250 mL of dimethylformamide (DMF) in a round-bottom flask. The mixture was stirred under reflux for 16 h. The resulting brown precipitate was recovered by filtration and then washed twice with 50 °C DMF, twice with 50 °C ethanol, and once with H₂O prior to drying at 150 °C.³⁰ MIL-100 was synthesized by dissolving H₃BTC (1.68 g, 7.6 mmol) and NaOH (0.91 g, 22.8 mmol) in 24 mL of H2O. This solution was added dropwise to a solution of FeCl₂·4H₂O (2.26 g, 11.4 mmol) in 97 mL of H₂O. This mixture was stirred for 24 h under ambient conditions. The resulting orange precipitate was isolated through filtration, washed three times with water and once with ethanol, and dried under ambient conditions.³³ Fe-BTC was synthesized by dissolving H₃BTC (0.263 g, 1.2 mmol) and NaOH (0.15 g, 3.8 mmol) in 10 mL of H₂O. This solution was added dropwise to a solution of FeCl₃·6H₂O (0.513 g, 1.9 mmol) in 10 mL of H_2O . This mixture was stirred for 10 min under ambient conditions, and the resulting orange precipitate was isolated, washed three times with water and once with ethanol, and dried under ambient conditions.³⁴ Fh was synthesized by adding 1 M NaOH dropwise to FeCl₃·6H₂O (5.4 g, 20.0 mmol) dissolved in 100 mL of H₂O until the pH reached ~7.5. The solid was isolated by centrifugation, washed with water (3× at 25 °C for 10 min), and lyophilized immediately following washing for 48 h.35 All frameworks and Fh were characterized by powder X-ray diffraction (PXRD), which matched previous literature reports.

Strains and Culture Conditions. All anaerobic cultures and experiments were performed inside a humidified Coy anaerobic chamber (3% $\rm H_2/balance~N_2$ atmosphere). S. oneidensis MR-1 was obtained from ATCC (700550). The mutant strain, $\Delta mtrC\Delta omcA\Delta mtrF$ (JG596), was generously provided by JA Gralnick (University of Minnesota, Minneapolis, MN). For anaerobic pregrowths, all strains were cultured in a Shewanella basal medium (SBM) buffered with 100 mM N-(2-hydroxyethyl)piperazine-N'ethanesulfonic acid and supplemented with 0.05% casamino acids and 1× Wolfe's mineral mix. The medium was adjusted to a pH of ~7.2. For pregrowths, sodium lactate (20 mM) and sodium fumarate (40 mM) were added as the carbon source and the electron acceptor, respectively. Once the bacteria reached stationary phase (ca. 18 h), they were pelleted by centrifugation (6000g; 20 min) and washed with NaHCO₃ buffer (30 mM, pH = 6.9) two times.

Growth of S. oneidensis MR-1 on MIL-127. Growth of S. oneidensis MR-1 on MIL-127 was measured by colony-forming unit (CFU) counts. Cultures containing 20 mM sodium lactate and MIL-127 ([Fe(III)] = 10 mM) in fresh SBM were prepared anaerobically and then inoculated with washed S. oneidensis MR-1. CFU studies used an inoculating value of $OD_{600} = 0.002$. Abiotic samples were prepared with the materials in SBM with lactate but with no cells. The cultures were incubated anaerobically at 30 °C. For CFU counting, an aliquot of the culture suspension was removed and serially diluted (10^1 to 10^6). Each dilution ($100~\mu$ L) was plated onto Luria Broth (LB) agar plates using sterile glass beads and incubated aerobically at 30 °C overnight. Individual colonies on each plate were counted, and the initial concentration of S. oneidensis MR-1 was calculated. Experiments were performed in triplicate.

Reduction of MIL-127 by S. oneidensis MR-1. Reduction of MIL-127 by S. oneidensis MR-1 was tested by measuring Fe(II) concentrations in framework—bacteria suspensions over time. Suspensions containing 20 mM sodium lactate and MIL-127 ([Fe(III)] = 10 mM) in fresh SBM were prepared anaerobically and then inoculated with washed MR-1 (OD $_{600}$ = 0.002 or 0.2). Abiotic samples were prepared with the materials in SBM with lactate but no cells. The suspensions were incubated anaerobically at 30 °C. At each time point, the suspensions were gently shaken to suspend the materials prior to removing an aliquot from the cultures. Each aliquot was mixed with 12 M HCl in a 1:1 ratio to achieve dissolution of the framework. If the Fe(II) concentrations were sufficiently large, the

sample was further diluted with $\rm H_2O$. All samples were analyzed for $\rm Fe(II)$ using the ferrozine assay. The ferrozine assay was performed by mixing 15 $\mu \rm L$ of the diluted sample with 235 $\mu \rm L$ of ferrozine solution in a 96-well plate. Absorbance was measured at 562 nm using a BMG LabTech CLARIOstar monochromator microplate reader. The ferrozine solution was prepared by mixing ferrozine (45 mg, 87 $\mu \rm mol$) and ammonium acetate (22.5 g, 0.29 mol) in 45 mL of $\rm H_2O$. Rates of iron reduction were calculated using linear squares regression analysis and were normalized by the sample's corresponding total protein biomass, as measured by the Bradford assay. Because of the interference between MIL-127 and the Bradford assay, total protein was measured in the reserved inoculum. Experiments were performed in triplicate.

Removal of Au(III). Au(III) removal was determined by adding Au(III) to pre-reduced cultures of S. oneidensis and its substrates. Prereduced cultures were obtained by inoculating stationary-phase S. oneidensis (OD₆₀₀ = 0.2) into suspensions of 20 mM lactate and either Fh, Fe-BTC, MIL-100, or MIL-127 ($[Fe(III)]_0 = 10 \text{ mM}$) in 30 mM bicarbonate buffer. Au(III) removal was also tested in cultures of S. oneidensis and fumarate. Stationary-phase S. oneidensis ($OD_{600} = 0.2$) was inoculated into a solution of 20 mM lactate and 40 mM lactate in 30 mM bicarbonate buffer. Abiotic samples were prepared with the substrates and bicarbonate buffer with lactate but with no cells. The cultures were incubated anaerobically at 30 °C for 24 h before a Au(III) ([Au(III)]₀ = 0.5 mM) challenge was added to each culture. After the addition of Au(III), the cultures were stored anaerobically at 30 °C for the duration of the experiment (up to 24 h). At each time point, an aliquot of the culture was removed and pelleted by centrifugation (11000g, 60 s). The resulting supernatant was diluted within the linear range of quantification (4-500-fold) using Milli-Q H_2O_2 , and 100 μ L of the diluted supernatant was mixed with 20 μ L of the TMB assay solution (2.0 mmol TMB in 4:1 solution of ethanol and NaAc/HAc, pH = 3.5 buffer) in a 96-well plate. The samples were incubated in the dark at room temperature for 3 min prior to measuring absorbance ($\lambda = 654$ nm) using a CLARIOstar monochromator microplate reader.³⁹ Rate constants for cultures with materials were determined from kinetic data by fitting to an exponential decay model for individual replicates using the following equation

$$C_x = (C_0 - a) e^{-kx} + a$$
 (1)

where x is the time, C_x is the Au(III) concentration at time x, C_0 is the initial concentration of Au(III), a is the plateau of the Au(III) concentration, and k is the rate constant. Fe(III) reduction in the cultures prior to Au(III) challenges was quantified using the ferrozine assay. For cultures containing MIL-100 or MIL-127, cell viability was assessed prior to and following a Au(III) challenge. For CFU counting, an aliquot of the culture suspension was removed and serially diluted (10^1 to 10^6). Dilutions ($100~\mu$ L) were plated onto LB agar plates using sterile glass beads and incubated aerobically at $30~^{\circ}$ C overnight. Individual colonies on each plate were counted, and the initial concentration of S. oneidensis MR-1 was calculated. Sampling occurred immediately following inoculation, immediately prior to the Au(III) challenge, and 4 h following the addition of Au(III). Experiments were performed in triplicate.

Maximum removal of Au(III) by each material was determined by challenging pre-reduced cultures of S. oneidensis and material with 5 mM Au(III). Pre-reduced cultures were obtained by inoculating stationary-phase S. oneidensis (OD₆₀₀ = 0.2) into suspensions of 20 mM lactate and either Fh, Fe-BTC, MIL-100, or MIL-127 ([Fe(III)]₀ = 10 mM) in 30 mM bicarbonate buffer. Abiotic samples were prepared with the substrates and bicarbonate buffer with lactate but with no cells. The cultures were incubated anaerobically at 30 °C for 24 h before a 5.0 mM Au(III) challenge was added to each culture. After the addition of Au(III), the cultures were stored anaerobically at 30 °C. After 24 h, the Au(III) in the supernatant was quantified and used to calculate the adsorption capacity, Q (mg g^{-1}), using the following equation

$$Q = \frac{(C_0 - C_f)V}{m} \tag{2}$$

where C_0 is the initial concentration of Au(III), C_f is the Au(III) concentration after 24 h, V is the volume of the culture, and m is the mass of the substrate. Experiments were performed in triplicate.

Cellular Reduction of Au(III). Biological reduction of Au(III) in the absence of the material was assessed by mixing cultures of 20 mM lactate and stationary-phase *S. oneidensis* MR-1 (inoculating OD₆₀₀ = 0.2) in 30 mM bicarbonate buffer with 100 μ M Au(III). The Au(III) concentration was monitored over the course of 4 h using the TMB assay. To determine the toxicity of Au(III) to *S. oneidensis* in a bicarbonate buffer, cultures containing 20 mM lactate in 30 mM bicarbonate buffer and inoculated with stationary-phase cells (OD₆₀₀ = 0.2) were challenged with either 0, 25, 50, or 100 μ M Au(III). Cell concentration was monitored using CFU counts. Experiments were performed in triplicate.

Au(III) Removal by Mutant-Reduced MIL-127. Au(III) removal by a mutant strain of *S. oneidensis* (JG596, $\Delta mtrC\Delta omcA\Delta mtrF$)-reduced MIL-127 was determined by adding Au(III) ([Au(III)] $_0$ = 0.5 mM) after 24 h of material reduction. Pre-reduced cultures were obtained by inoculating stationary-phase *S. oneidensis* JG596 (OD $_{600}$ = 0.2) into suspensions of 20 mM lactate and MIL-127 ([Fe(III)] $_0$ = 10 mM) in 30 mM bicarbonate buffer. Abiotic samples were prepared with the substrates and bicarbonate buffer with lactate but with no cells. The cultures were incubated anaerobically at 30 °C for 24 h before a 0.5 mM Au(III) challenge was added to each culture. After the addition of Au(III), the cultures were stored anaerobically at 30 °C for the duration of the experiment (4 h). Au(III) concentration was measured using the TMB assay, while Fe(II) concentration was measured using the ferrozine assay. Experiments were performed in triplicate.

Au(III) Removal by Non-viable Cells. Au(III) removal by non-viable *S. oneidensis* MR-1 in the presence of reduced MIL-127 was determined by heat-treating cells following the pre-reduction. Pre-reduced cultures were obtained by inoculating stationary-phase *S. oneidensis* (OD₆₀₀ = 0.2) into suspensions of 20 mM lactate and MIL-127 ([Fe(III)]₀ = 10 mM) in 30 mM bicarbonate buffer. Abiotic samples were prepared with the substrates and bicarbonate buffer with lactate but with no cells. The cultures were incubated anaerobically at 30 °C for 24 h before the heat-killed suspensions were heated at 80 °C for 10 min anaerobically. Heat-killed suspensions were transferred to sterile culture tubes after heating. Then, all samples were challenged with 0.5 mM Au(III), and Au(III) concentrations were monitored using the TMB assay and Fe(II) concentrations using the ferrozine assay. Experiments were performed in triplicate.

Au(III) Cycling. Cycling with Au(III) was performed by challenging pre-reduced cultures of S. oneidensis MR-1 and either MIL-100 or MIL-127 with repeated additions of Au(III) ([Au(III)]₀ = 0.5 mM). Pre-reduced cultures were obtained by inoculating stationary-phase S. oneidensis (OD₆₀₀ = 0.2) into suspensions of 20 mM lactate and either MIL-100 or MIL-127 ($[Fe(III)]_0 = 10 \text{ mM}$) in 30 mM bicarbonate buffer. Abiotic samples were prepared with the substrates and bicarbonate buffer with lactate but with no cells. The cultures were incubated anaerobically at 30 °C for 24 h prior to the first 0.5 mM Au(III) challenge. Following the Au(III) challenge, the cultures were allowed to regenerate Fe(II) between 24 and 48 h before the next addition of Au(III). MIL-100 underwent three cycles, while MIL-127 underwent five cycles. Between cycle four and five for MIL-127, cell viability was tested by plating an undiluted aliquot of the cultures on LB agar plates. Plated cells were incubated aerobically at 30 °C overnight before assessing for CFUs. Au(III) concentrations were measured 10 min after each addition and used to calculate percent removal, which was defined as

% removal =
$$\frac{C_0 - C_f}{C_0} \times 100\%$$
 (3)

where C_0 is the initial $\mathrm{Au}(\mathrm{III})$ concentration and C_f is the $\mathrm{Au}(\mathrm{III})$ concentration in the supernatant 10 min after addition. Fe(II)

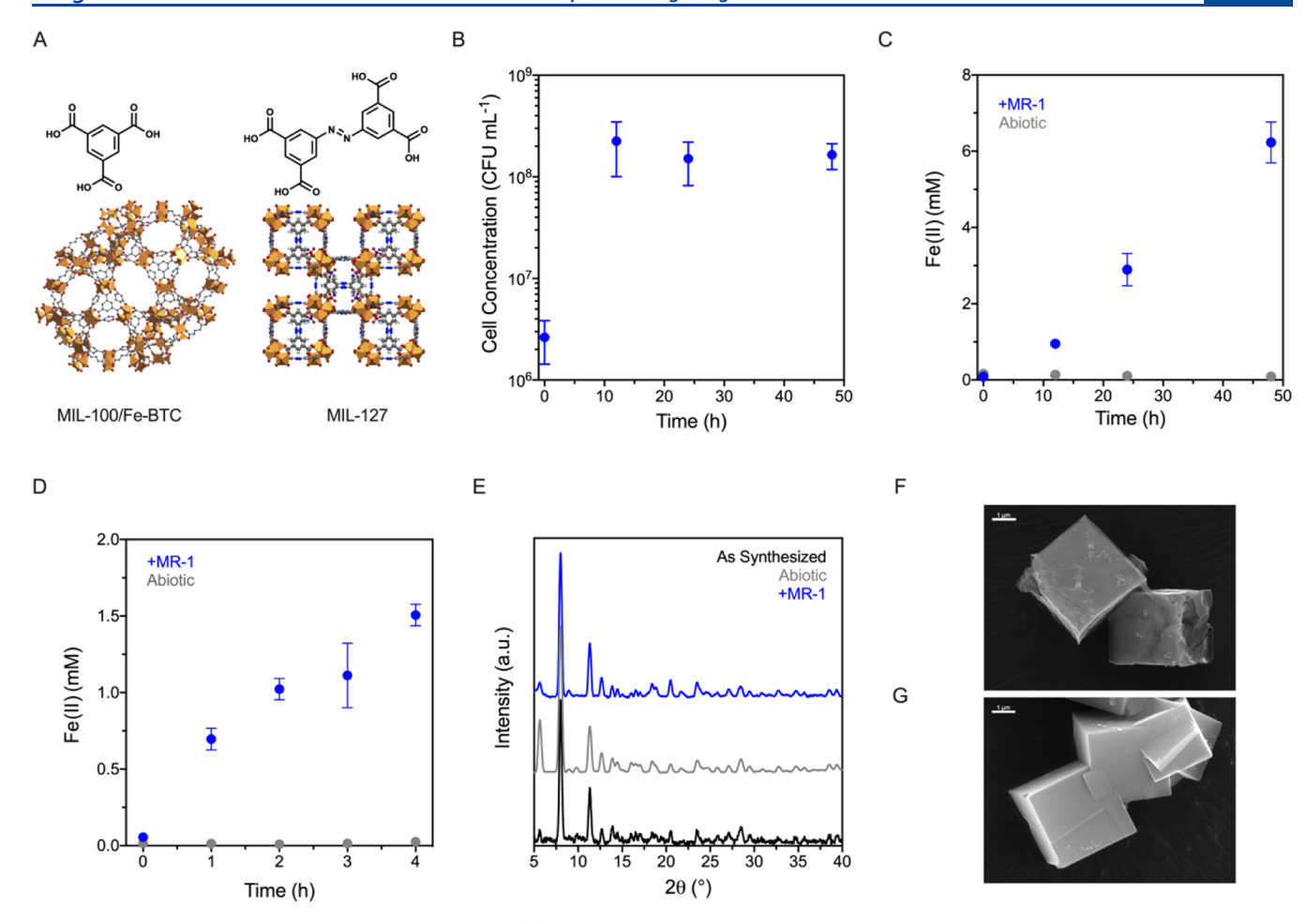


Figure 1. Reduction of MIL-127 by *S. oneidensis* MR-1. (A) Comparison of the structures and ligands of MIL-100/Fe-BTC, a known *S. oneidensis* substrate, with that of MIL-127. (B) Concentration of viable *S. oneidensis* MR-1 cells grown on MIL-127 in SBM. The inoculating was OD₆₀₀ = 0.002. (C) Fe(II) concentrations of cultures of *S. oneidensis* (inoculating OD600 = 0.002) in SBM with 20 mM lactate and MIL-127 (blue). The abiotic control is shown in gray. These data were collected concomitantly with growth (as measured by CFU counts) shown in (B). (D) Reduction of Fe(III) by *S. oneidensis* MR-1 (blue) with MIL-127 as an electron acceptor and SBM as the culture medium (inoculating OD₆₀₀ = 0.2). The abiotic control containing only MIL-127 in the culture medium is shown in gray. (E) PXRD spectra of MIL-127 as-synthesized (black) and after 24 h of reduction by *S. oneidensis* (blue). The abiotic control is shown in gray. (F,G) SEM imaging of MIL-127 after 24 h of reduction by *S. oneidensis* (F) and of the abiotic control (G). Scale bars are 1 μ m. Data shown are mean \pm SD for three independent biological replicates.

concentrations were monitored using the ferrozine assay before each Au(III) cycle. Experiments were performed in triplicate.

Electron Microscopy. Scanning electron microscopy (SEM) and elemental mapping were used to image the metal—organic frameworks and the extent of Au(III) adsorption. Images were collected using an FEI Quanta 650 ESEM apparatus equipped with a Bruker EDX system. Framework samples were washed 3× with Milli-Q water and 3× with ethanol and dried anaerobically at 30 °C. Dried samples were prepared on carbon-taped mounts and coated with Pd/Au at 40 mA for 40 s using a Denton Thermo sputter coater. Samples analyzed for elemental mapping were not sputter-coated. Esprit software was used analyze the normalized weight and atomic percentage of Fe and Au in the cycled frameworks and to generate elemental mapping images.

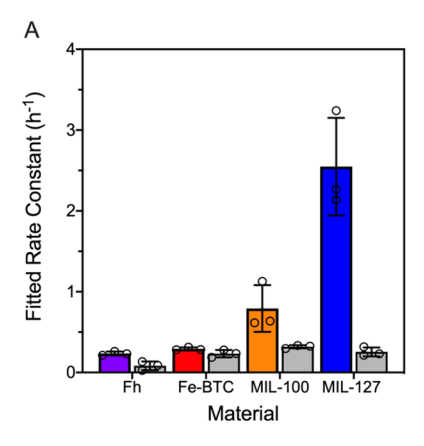
Statistical Analysis. Data are reported as mean \pm standard deviation (SD) of N=3 biological replicates as this sample size was sufficiently large to detect significant differences in means. Significance was calculated using an unpaired two-tailed Student's t-test ($\alpha=0.05$) or analysis of variance with post-hoc Tukey's test in Prism 8 by GraphPad Software (San Diego, CA). Calculation of replicate rate constants was performed by using least-squares regression with a weighting of $1/y^2$. All fitting was performed in Prism 8.

■ RESULTS AND DISCUSSION

MIL-127 Supports Microbial Growth and Reduction.

We previously established that MIL-100 and Fe-BTC could be used as substrates for *S. oneidensis* growth. Similar to these frameworks, MIL-127 contains Fe(III) nodes, which could act as an electron sink for *S. oneidensis* respiration. Instead of a trimesate organic linker, MIL-127 contains the azo-based ligand H₄TazBz (Figure 1A). This changes the properties of the framework, resulting in particle morphologies, particle sizes, and surface areas that matched literature reports but are distinct from those of MIL-100 and Fe-BTC.^{30,41,42} In particular, SEM images of MIL-127 reveal cubic-shaped particles (Figure S1), as opposed to the octahedron-shaped particles of MIL-100.⁴³ Because particle morphology and surface areas of metal—organic frameworks might impact framework use as a microbial growth substrate,²² we first asked if MIL-127 could be reduced by *S. oneidensis* and could support its growth.

Prior to examining growth trends, the stability of MIL-127 ([Fe(III)] = 10 mM) was examined under abiotic culture conditions. The framework was exposed to SBM containing 20 mM lactate at 30 $^{\circ}$ C under anaerobic conditions. After 48 h of



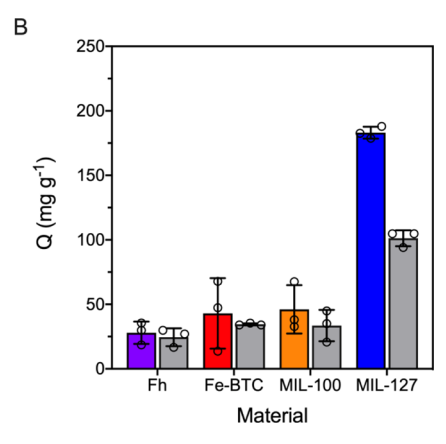


Figure 2. Removal of Au(III) by *S. oneidensis*-reduced substrates. (A) The fitted rate constants (k) for the removal of Au(III) from the supernatant by mixtures containing *S. oneidensis* and Fh (purple), Fe-BTC (red), MIL-100 (orange), or MIL-127 (blue). Cells (inoculating OD₆₀₀ = 0.2) were pre-grown on each substrate for 24 h in 30 mM bicarbonate-buffered medium prior to the addition of 0.5 Au(III). All abiotic treatments are shown in gray. (B) Maximum removal capacity (Q) of *S. oneidensis* MR-1 + material suspensions when challenged with 5 mM Au(III). Cells (inoculating OD₆₀₀ = 0.2) were pre-grown on each substrate for 24 h in 30 mM bicarbonate-buffered medium prior to the addition of Au(III). All abiotic treatments are shown in gray. Data shown are mean \pm SD for three independent biological replicates.

exposure, only 0.14 ± 0.02 mM total Fe had leached from the framework, meaning that 98.6% of Fe(III) remained in the framework (Figure S2). Furthermore, PXRD patterns of the exposed framework did not show any difference from that of the as-synthesized framework (Figure S3). These data indicate that MIL-127 is stable in a buffer typically used to support S. oneidensis growth.

To monitor the growth of S. oneidensis on MIL-127, the material was suspended in SBM containing lactate as the carbon source and inoculated with lag-phase cells (OD_{600} = 0.002). CFUs from plated dilutions of the material-bacteria suspension were used to measure the cell concentration. For MIL-127, we observed an increase in the cell concentration after 12 h that remained constant up to 48 h (Figure 1B). These data were comparable to growth trends previously observed with MIL-100 and iron oxides.^{22,44} The growth of S. oneidensis occurred concomitantly with an increase in the Fe(II) concentration (Figure 1C). Unfortunately, biomassnormalized Fe(III) reduction rates could not be obtained for reduction by lag-phase cells due to the interference of MIL-127 with Coomassie staining of the protein biomass. To address this limitation, cultures of MIL-127 were inoculated with stationary-phase cells ($OD_{600} = 0.2$) and protein biomass was assessed from the stocks of the inocula. Protein levels of these stationary-phase inocula were consistent with previously measured biomass levels following S. oneidensis growth on MIL-100 and Fh.²² Under these conditions, we observed a steady increase in the concentration of Fe(II) in MIL-127 suspensions (Figure 1D), with a biomass-normalized reduction rate of 3.90 \pm 0.68 μ mol mg⁻¹ h⁻¹.

Similar to metal oxides, we previously showed microbially reduced metal—organic frameworks release Fe(II) into solution. Despite the release of some Fe(II), the frameworks remained crystalline with reduced Fe contained in the structure. To determine if MIL-127 behaved similarly, the amounts of Fe(II) in the framework and in the supernatant were measured following 24 h of reduction (inoculating $OD_{600} = 0.002$). We observed that approximately 31% of the total Fe(II) was contained in the framework following reduction. The remaining Fe(II) had been released into the supernatant (Figure S4). The amount of Fe(II) contained in MIL-127 particles was less than that of MIL-100, meaning that MIL-127

was less able to stabilize the influx of electrons. However, the crystalline structure of MIL-127 was still intact following 24 h of reduction, as confirmed by PXRD, SEM imaging, and infrared spectroscopy (IR) analysis (Figures 1E–G and S5).

Taken together, these data indicate that MIL-127 can act as a microbial growth and reduction substrate, which expands the range of materials available for biological reduction-based applications. The amount of Fe(II) that is produced through this biological reduction process is substantial, with biomass-normalized reduction rates and amounts exceeding those observed for MIL-100 and Fe-BTC under similar conditions (Figure S6).²² Despite the lower amount of Fe(II) in the framework, the relatively large total Fe(II) concentrations can be exploited to improve adsorption processes that leverage redox transformations of pollutants or metals of interest.

Remediation of Au(III). Redox-based transformations play important roles in the separation of metals from solutions, with Fe(II) being of particular significance. It has previously been shown that a pathway for the adsorption of Au(III) can involve the redox reaction with Fe(II), which produces Fe(III) and Au^0 . Indeed, we observed that the addition of soluble Fe(II) exhibited the reduction of approximately one-third of the available Au(III) after 4 h under our conditions, adhering to the expected reaction stoichiometry (Figure S7)

$$3Fe^{2+} + Au^{3+} \rightarrow 3Fe^{3+} + Au^{0}$$
 (4)

This reaction can also occur with Fe(II)-bearing minerals or solubilized Fe(II) that originates from the dissolution of such minerals. Similar to these iron oxides, reduced iron-based metal—organic frameworks can incorporate Fe(II) into their structures, 22,23 possibly improving their adsorption properties for Au(III). Having determined that the reduction of MIL-127 by S. oneidensis produces large amounts of Fe(II), we next examined the efficacy of this microbe—material pairing for the adsorption of Au(III) from solutions. We also compared its performance with that of other redox-active materials that are reduced by microbes to a lesser extent, namely, the frameworks MIL-100 and Fe-BTC and the model iron oxide Fh.

In initial experiments, we inoculated suspensions of MIL-127, MIL-100, Fe-BTC, or Fh ([Fe(III)] = 10 mM), 20 mM lactate, and 30 mM bicarbonate-buffered medium with stationary-phase cells (OD $_{600}$ = 0.2). The bicarbonate-buffered

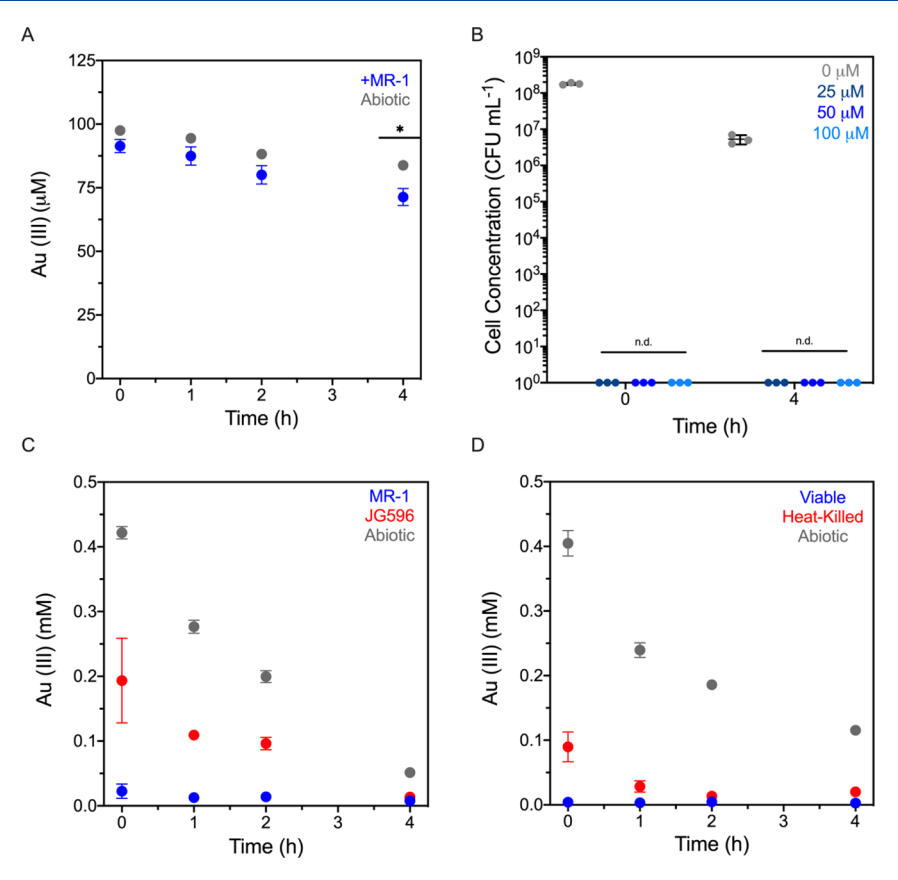


Figure 3. Biological contributions to Au(III) removal. (A) Removal of 100 μ M Au(III) from the supernatant by cultures containing *S. oneidensis* MR-1 (blue) as compared to that by an abiotic control (gray). All samples contained no material. *P=0.02. (B) Concentration of viable *S. oneidensis* MR-1 cells in 30 mM bicarbonate-buffered medium exposed to 0 μ M Au(III) (gray), 25 μ M Au(III) (dark blue), 50 μ M Au(III) (blue), and 100 μ M Au(III) (light blue). The inoculating density was OD₆₀₀ = 0.2. All samples contained no material. For t=0 h, n.d. refers to a CFU concentration below the limit of detection (10⁶ CFU mL⁻¹). For t=4 h, n.d. refers to a CFU concentration below the limit of detection (10² CFU mL⁻¹). (C) Removal of 0.5 mM Au(III) from the supernatant by a suspension of MIL-127 and wild-type *S. oneidensis* MR-1 (blue) or the Δ $mtrC\Delta omcA\Delta mtrF$ mutant strain JG596 (red). Cells (inoculating OD₆₀₀ = 0.2) were pre-grown on MIL-127 for 24 h in 30 mM bicarbonate-buffered medium prior to the addition of Au(III). The abiotic treatment is shown in gray. (D) Removal of 0.5 mM Au(III) from the supernatant by a suspension of MIL-127 and viable (blue) or heat-killed *S. oneidensis* MR-1 (red). Cells (inoculating OD₆₀₀ = 0.2) were pre-grown on MIL-127 for 24 h in 30 mM bicarbonate-buffered medium. Prior to challenging the cultures with Au(III), the heat-killed samples were heated at 80 °C to suspend metabolic activity while maintaining Fe(II) in the structure of MIL-127. The abiotic treatment is shown in gray. Data shown are mean ± SD for three independent biological replicates.

medium was chosen to reduce the effect of the promiscuous reduction of Au(III), which occurs in common microbial buffers including SBM and LB. As controls, we examined abiotic suspensions of each material, as well as cells in the absence of an iron-based adsorbent material, instead substituting 40 mM fumarate as the growth substrate. After 24 h of reduction, each biotic or abiotic sample was challenged with an addition of 0.5 mM Au(III), after which the concentrations of Au(III) and Fe(II) were monitored. For the fumarate controls, there was no significant removal of Au(III) and no difference between the abiotic and biotic samples after 24 h (Figure S8). Likewise, Fh, MIL-100, and Fe-BTC exhibited comparable Au(III) removal between biotically reduced samples and abiotic treatments. In contrast, we observed that biotically reduced MIL-127 exhibited a drastic improvement in Au(III) removal relative to that of the abiotic treatment. Within minutes of the addition of 0.5 mM Au(III) to cultures of MIL-127 and S. oneidensis, only 59 μ M Au(III) remained in the solution, corresponding to a percentage removal of 88.1%. After 2 h, the supernatant concentration of Au(III) had decreased to 1.7 μ M (99.7% removal). To further analyze the rates of Au(III) removal, the kinetic data of Au(III)

removal for all material-containing suspensions were fitted to an exponential decay model, and rate constants were obtained. Obtained. Supporting our raw kinetic trends, S. oneidensis-reduced MIL-127 displayed the highest rate constant ($k = 2.55 \pm 0.60 \text{ h}^{-1}$), followed by S. oneidensis-reduced MIL-100 ($k = 0.79 \pm 0.29 \text{ h}^{-1}$; Figure 2A; Tables S1 and S2). However, all abiotic treatments, as well as biotically reduced suspensions of Fe-BTC and Fh, featured relatively low rate constants. Collectively, these data show that MIL-127 exhibits the fastest Au(III) removal rates.

We also examined the maximum capacity of each of the microbially reduced materials by challenging cultures with a single dose of 5 mM Au(III). After 24 h, we found that MIL-100, Fe-BTC, and Fh had adsorbed only small amounts of Au(III) (Figure 2B; Table S3). Additionally, none of these materials exhibited significant differences between the abiotic and biotic treatments. This was in contrast to MIL-127, which displayed a nearly 2-fold increase in the maximum adsorption capacity for the biotically reduced samples as compared to that for the abiotic treatment. The reduced MIL-127 samples also displayed the highest adsorption capacity of the materials we tested, having removed 183 mg Au per gram of the material.

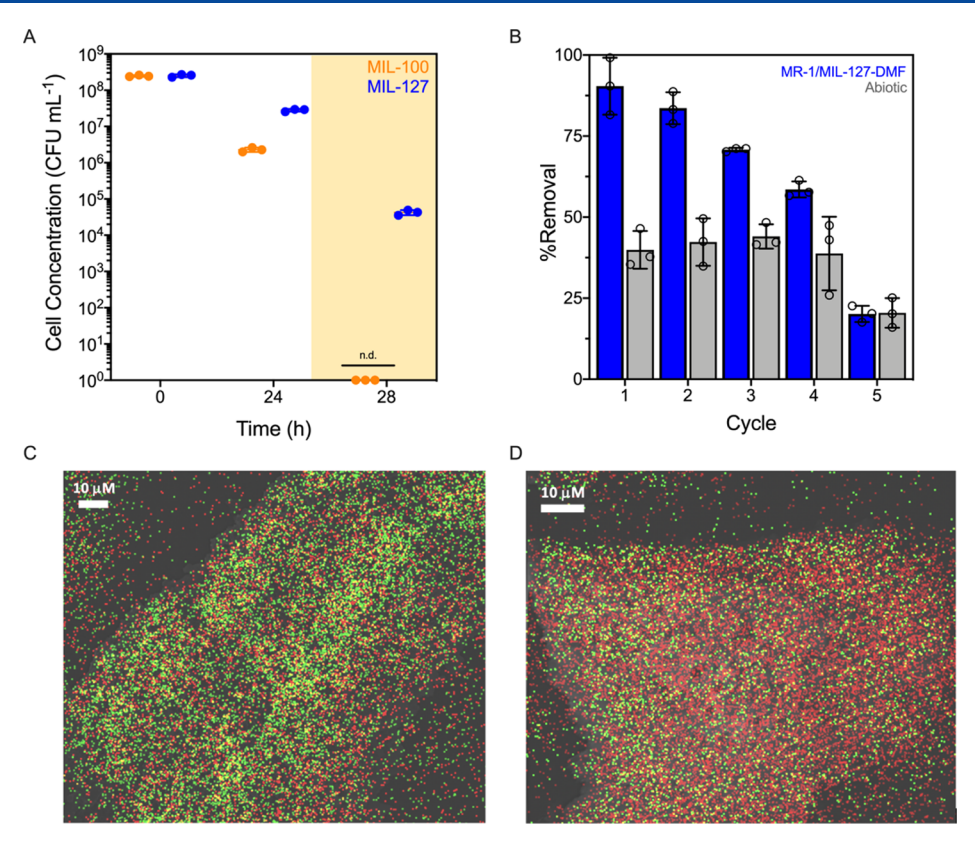


Figure 4. Cycling performance of *S. oneidensis*-reduced MIL-127. (A) Concentration of viable *S. oneidensis* MR-1 cells grown on MIL-100 (orange) or MIL-127 (blue) in 30 mM bicarbonate-buffered medium at inoculation (0 h), after 24 h of reduction but before the Au(III) challenge, and 4 h after the addition of a 0.5 mM Au(III) challenge (28 h). Cells (inoculating OD₆₀₀ = 0.2) were pre-grown on MIL-127 for 24 h in 30 mM bicarbonate-buffered medium prior to the addition of Au(III). n.d. refers to a CFU concentration below the limit of detection (10² CFU mL⁻¹). (B) Percent removal for each 0.5 mM Au(III) cycle by suspensions of *S. oneidensis* MR-1 and MIL-127 (blue). Cells (inoculating OD₆₀₀ = 0.2) were pre-grown on MIL-127 for 24 h in 30 mM bicarbonate-buffered medium prior to the first addition of Au(III). Cells were allowed to reduce MIL-127 to accumulate Fe(II) in the suspension before subsequent cycles of Au(III). Abiotic samples are shown in gray. (C,D) EDX element mapping of (C) *S. oneidensis* MR-1-reduced MIL-127 and (D) abiotic MIL-127 following five Au(III) cycles. Fe is shown in red and Au is shown in green. Scale bars are 10 μm. Data shown are mean ± SD for three independent biological replicates.

This value compares favorably with the performance of other sorbent materials at circumneutral pH (ca. 3.58-350 mg Au g^{-1}). $^{47-50}$

The concentrations of Fe(II) match closely with the materials' efficacy of Au(III) removal, which suggests that the amount of Fe(II) may be the dominant factor in controlling Au(III) adsorption. Due to different extents of microbial reduction, MIL-127 contained the most Fe(II) amount, while Fh contained the lowest amount of Fe(II) (Figure S9). Likewise, we observed that MIL-127 had the highest adsorption capacity and removal rate. However, the Fe(II)-driven removal effects observed in MIL-127 may also have been enhanced by its azo-based ligand, H₄TazBz. Relative to the trimesate linker in MIL-100, we observed that soluble H₄TazBz demonstrated higher reduction of Au(III) in the absence of cells (Figure S10). This improved performance of H₄TazBz over that of trimesate may be due a small amount of amine impurity present in H₄TazBz, which we were unable to completely remove via recrystallization (Figure S11). Although the exact mechanism remains unclear, azo-containing compounds, such as chemical dyes, can be degraded by various Shewanella species. 52 Indeed, we observed the disappearance of the azo peak (1580 cm⁻¹) in the IR spectrum of reduced MIL-127 (Figure S5), indicating that biological reduction of the framework ligand could be another contributor to Au(III)

reduction and a key difference between MIL-127 and other tested frameworks.

Biological Contribution to Au(III) Removal. While we hypothesized that the chemical components of the metalorganic frameworks were predominantly responsible for the reduction of Au(III), we also considered that the biological component, namely, *S. oneidensis* MR-1, may also play a role in this process. It has been previously found that *S. oneidensis* can form Au nanoparticles through the reduction of Au(III), though this process does not appear to be tied to the Mtr extracellular reduction pathway. ^{53,54} As such, the bacteria may be aiding the reduction of Au(III) in addition to Fe(II) contained in reduced MIL-127.

To test this, we first examined the ability of *S. oneidensis* MR-1 to reduce Au(III) in the absence of a material. We challenged cultures of stationary-phase *S. oneidensis* ($OD_{600} = 0.2$) in bicarbonate-buffered medium with 100 μ M Au(III). Even though this challenge was considerably lower than what was used with material suspensions, we noted that the cells had significantly lower Au(III) concentrations after 4 h as compared to the abiotic control (Figure 3A). However, the amount reduced was relatively small compared to the initial dose. To determine if this small amount of removal was due to a lack of viable cells, we performed colony counts with cell cultures exposed to Au(III) concentrations of up to 100 μ M (Figure 3B). For all non-zero concentrations of Au(III), we

found considerable toxicity effects, with all CFU counts falling below the limit of detection (10^2 CFU mL⁻¹) after 4 h. We also found that cell viability decreased in the absence of an electron acceptor [0 μ M Au(III)] under our conditions, but this effect was not as severe (Figure 3B). While other studies have not found toxicity effects for a Au(III) concentration of up to 75 μ M in LB medium,⁵³ the medium composition likely exerts a large effect on cell viability and function due to abiotic Au(III) reduction. Given the compromised viability of *S. oneidensis* and the minimal removal of Au(III), these data collectively support a diminished role of cellular reduction in the bicarbonate buffer.

Despite the minimal role of direct cellular reduction of Au(III) in our system, our data suggest that metabolically active cells are still a critical component for effective removal. Based on the high efficacy of Fe(II)-mediated reduction of Au(III), we hypothesized that generation of Fe(II) by S. oneidensis EET was the dominant biological contribution. To confirm this, we compared Au(III) removal between MIL-127 reduced by wild-type S. oneidensis and that by a mutant strain with attenuated Fe(III)-reduction capabilities ($\Delta mtrC\Delta om$ $cA\Delta mtrF$). As expected, we found that this knockout strain produced a lower concentration of Fe(II) relative to the wild type strain (Figure S12). Supporting our hypothesis, we also observed a decreased amount of Au(III) removed at initial time points with this strain as compared to that with wild-type cells (Figure 3C). Furthermore, we assessed whether the metabolic activity was required during Au(III) removal by heat-killing cells after reducing MIL-127 but prior to Au(III) exposure. While the process of heat treatment slightly altered Fe(II) concentrations,⁵⁵ significant quantities of Fe(II) remained in the cultures (Figure S13). We observed that the heat-treated suspensions removed Au(III) to a similar extent to that removed by viable cell controls (Figure 3D). Together, these experiments highlight the importance of microbial generation of Fe(II) for efficacious Au(III) removal in our

Au(III) Cycling. Notably, for viable cell treatments grown on MIL-127, we observed that Fe(II) generation continued after a Au(III) challenge. When post-challenge colony counts were assessed, we indeed found that cell viability persisted (Figure 4A). This observation suggested that MIL-127 affords some protection to normally toxic Au(III) concentrations and that our system may be able to treat repeated challenges of Au(III). To test this, we pre-grew S. oneidensis MR-1 (inoculating $OD_{600} = 0.2$) with MIL-127 in 30 mM bicarbonate buffer for 24 h prior to introducing the first 0.5 mM Au(III) challenge. We subsequently added multiple challenges of 0.5 mM Au(III). As Fe(II) is one of the dominant reductants of Au(III) in our system, we allowed the cells to generate more Fe(II) in between the additions of Au(III). Under these conditions, we found that up to five cycles of Au(III) removal could be performed (Figure 4B). Removal efficiency remained between 55 and 99% for the first four cycles but decreased to ca. 20% at cycle five. This contrasts with abiotic treatments where percent removal remained below 50% across all cycles (Figure 4B). EDX element mapping confirmed the increased presence of Au as compared to that of Fe in the biotically reduced MIL-127 as compared to that in the abiotic treatment (Figure 4C,D). Based on these results, the presence of cells appears necessary for the improved cyclability efficiency.

While Fe(II) was consumed and biologically regenerated after each Au(III) addition (Figure S14), we observed that the extent of regeneration decreased with the increasing cycle number. Decreases in Fe(II) levels correlated with the decrease in the percent removal. To further explore the impact of biologically generated Fe(II) on Au(III) cycling, we also examined suspensions of S. oneidensis MR-1 and MIL-100 (Figure S15). For these samples, poor percent removal was observed for the first cycle (ca. 22%), and it remained low for subsequent cycles. Relative to MIL-127, S. oneidensis MR-1 generated a lower concentration of Fe(II) in MIL-100 suspensions prior to the first Au(III) addition, and Fe(II) concentrations did not exhibit recovery following the initial cycle. Collectively, these data suggest that high levels of Fe(II) are important for maintaining high Au(III) removal percentages.

Our results show that pairing an electroactive bacterium with a redox-active metal—organic framework can significantly increase the Au(III) removal capacity of the material. When using the novel *S. oneidensis* substrate, MIL-127, we observed that the maximum capacity of the material nearly doubled in the presence of cells. Furthermore, we found that microbially reduced MIL-127 displayed a significantly faster rate of removal of Au(III) compared to other materials tested under our conditions, both abiotic and biotic. The near-complete removal of Au(III) by reduced MIL-127 within minutes appears to be driven by the substantial concentrations of microbially generated Fe(II).

CONCLUSIONS

Overall, our results highlight important considerations for Au(III) removal platforms, especially those that may incorporate a living, biological component. Under our conditions with a minimal medium (30 mM bicarbonate buffer), we found that cell viability was compromised when S. oneidensis was exposed to low concentrations of Au(III) (>25 μ M) in material-free cultures. However, when the cells were grown on MIL-127, they were able to survive a dose of Au(III) that was 20-fold higher. This suggests that the chemical characteristics of the metal-organic framework protected the cells from a normally lethal dose of Au(III). Specifically, high levels of Fe(II) appear to quickly reduce Au(III) and alleviate toxicity to the cells. When only low amounts of Fe(II) were generated, such as with cultures of S. oneidensis and MIL-100, the protective effects were no longer present. This was evidenced by the lack of Fe(II) regeneration following Au(III) cycles in MIL-100 cultures relative to MIL-127 cultures. Our results also suggest that framework ligands may play some role in the observed differences between MIL-100 and MIL-127, although further investigation is needed to determine mechanistic contributions to Au(III) reduction. With these observations in mind, future optimizations should focus on increasing the amount of generated Fe(II), either by maintaining cell viability or by controlling Fe(III) reduction rates. For example, altered growth medium composition may better support cell viability (e.g., rich medium) when exposed to Au(III).53 Separately, S. oneidensis genotypes exhibiting higher rates of Fe(III) reduction may exhibit improved resilience to Au(III) challenges under cycling conditions. Alternatively, different Fe(III)-based materials that support microbial growth/reduction could be leveraged to increase the Fe(III) reduction rate. For instance, we have shown that MIL-127 has a larger extent of Fe(II) produced as compared to previously used substrates, such as MIL-100 or Fh.²² Given the efforts to expand the diversity of metal—organic frameworks, ⁵⁶ future Fe(III)-containing frameworks may be designed to optimize biological reduction rates and push microbe/metal—organic framework Fe(II) generation into new applications (e.g., advanced oxidation processes).⁵⁷

In sum, this work demonstrates the potential for EET to improve redox-driven Au(III) extraction processes. While most material-oriented systems have focused on chemical tunability to improve the Au(III) removal performance, our work shows that electroactive microbes can enable biological tunability of these platforms as well. For example, metabolic and protein engineering strategies applied to the electron transfer pathway of *S. oneidensis* may further enhance Fe(III) reduction and Au(III) removal. Relative to purely chemical systems, the inclusion of biological components offers new opportunities for optimizing remediation schemes.

ASSOCIATED CONTENT

Supporting Information

The Supporting Information is available free of charge at https://pubs.acs.org/doi/10.1021/acs.langmuir.1c01180.

Materials and Methods; SEM of MIL-127; leaching of Fe(III) from MIL-127; PXRD of MIL-127 exposed to abiotic culture conditions; Fe(II) in reduced MIL-127; IR spectra of reduced MIL-127; Fe(II) in S. oneidensisreduced material suspensions; Au(III) reduction by soluble Fe(II); Au(III) removal by S. oneidensis-reduced substrates; fitted values of Au(III) reduction for Figure 2A; significant P values for fitted rate constants for Figure 2A; significant P values for Figure 2B; Fe(II) in S. oneidensis-reduced material suspensions; Au(III) reduction by framework ligands; structures of potential impurities in the H₄TazBz ligand; reduction of MIL-127 by an EET-deficient mutant; Fe(II) in MIL-127 suspensions after heat treatment; Fe(II) contained in MIL-127/MR-1 suspensions during Au(III) cycling; and removal of Au(III) by MIL-100 over cycles (PDF)

AUTHOR INFORMATION

Corresponding Author

Benjamin K. Keitz – McKetta Department of Chemical Engineering, University of Texas at Austin, Austin, Texas 78712, United States; orcid.org/0000-0003-3314-0053; Phone: +1 512-232-2373; Email: keitz@utexas.edu

Author

Sarah K. Springthorpe — Department of Chemistry, University of Texas at Austin, Austin, Texas 78712, United States;
orcid.org/0000-0002-6761-9399

Complete contact information is available at: https://pubs.acs.org/10.1021/acs.langmuir.1c01180

Author Contributions

The manuscript was written through contributions of all authors. All authors have given approval to the final version of the manuscript. S.K.S. and B.K.K. conceived and designed the experiments. S.K.S. performed the experiments, material synthesis, and characterization. B.K.K. supervised the project. All authors contributed to data analysis and the writing of the manuscript.

Notes

The authors declare no competing financial interest. Source data is available from the Texas Data Repository at https://doi.org/10.18738/T8/BRSVAW

ACKNOWLEDGMENTS

We thank Michael Lucas and Christopher Dundas for their experimental assistance. *S. oneidensis* strain JG596 was provided by Prof. Jeffrey Gralnick. We acknowledge the use of facilities within the core microscopy lab of the Texas Materials Institute, University of Texas at Austin, within the XRD Lab, University of Texas at Austin, and the Mass Spectrometry Facility, University of Texas at Austin. S.K.S. was supported through Provost's Graduate Excellence Fellowship (PGEF). This work was partially supported by the Welch Foundation (Grant F-1929), the National Institutes of Health under award number R35GM133640, and the National Science Foundation through the Center for Dynamics and Control of Materials: an NSF Materials Research Science and Engineering Center under DMR-1720595.

ABBREVIATIONS

EET, extracellular electron transfer; BTC, 1,3,5-benzenetricar-boxylate; MIL-100, Fe₃O(BTC)₂(OH)·nH₂O; MIL-127, Fe₃O(H₄TazBz)_{1.5}(H₂O)₃·nH₂O; H₄TazBz, 3,3′5,5′-azobenzenetetracarboxylic acid; NMR, nuclear magnetic resonance; LC–MS, liquid chromatography–mass spectrometry; H₃BTC, benzene-1,3,5-tricarboxylic acid; Fh, ferrihydrite; PXRD, powder X-ray diffraction; SBM, *Shewanella* basal medium; SEM, scanning electron microscopy; IR, infrared spectroscopy

REFERENCES

- (1) Zientek, M. L.; Loferski, P. J. Platinum-Group Elements—So Many Excellent Properties, Fact Sheet 2014-3064; USGS Mineral Resources Program, 2014; p 2.
- (2) U.S. Geological Survey. Mineral Commodity Summaries 2020, 2020; pp 1–200.
- (3) Zhang, S.; Ding, Y.; Liu, B.; Chang, C.-c. Supply and Demand of Some Critical Metals and Present Status of Their Recycling in WEEE. *Waste Manage.* **2017**, *65*, 113–127.
- (4) Wang, M.; Tan, Q.; Chiang, J. F.; Li, J. Recovery of Rare and Precious Metals from Urban Mines—A Review. *Front. Environ. Sci. Eng.* **2017**, *11*, 1–17.
- (S) Prichard, H. M.; Wedin, F.; Sampson, J.; Jackson, M. T.; Fisher, P. C. Precious Metals in Urban Waste. *Water Environ. J.* **2016**, *30*, 151–156
- (6) Vriens, B.; Voegelin, A.; Hug, S. J.; Kaegi, R.; Winkel, L. H. E.; Buser, A. M.; Berg, M. Quantification of Element Fluxes in Wastewaters: A Nationwide Survey in Switzerland. *Environ. Sci. Technol.* **2017**, *51*, 10943–10953.
- (7) McHugh, J. B. Concentration of Gold in Natural Waters. J. Geochem. Explor. 1988, 30, 85–94.
- (8) Kenison Falkner, K.; Edmond, J. M. Gold in Seawater. Earth Planet. Sci. Lett. 1990, 98, 208-221.
- (9) Lin, S.; Reddy, D. H. K.; Bediako, J. K.; Song, M.-H.; Wei, W.; Kim, J.-A.; Yun, Y.-S. Effective Adsorption of Pd(Ii), Pt(Iv) and Au(Iii) by Zr(Iv)-Based Metal—Organic Frameworks from Strongly Acidic Solutions. *J. Mater. Chem. A* **2017**, *5*, 13557—13564.
- (10) Lin, S.; Bediako, J. K.; Cho, C.-W.; Song, M.-H.; Zhao, Y.; Kim, J.-A.; Choi, J.-W.; Yun, Y.-S. Selective Adsorption of Pd(II) over Interfering Metal Ions (Co(II), Ni(II), Pt(IV)) from Acidic Aqueous Phase by Metal-Organic Frameworks. *Chem. Eng. J.* **2018**, 345, 337–344.

- (11) Kim, S.; Song, M.-H.; Wei, W.; Yun, Y.-S. Selective Biosorption Behavior of Escherichia Coli Biomass toward Pd(II) in Pt(IV)—Pd(II) Binary Solution. *J. Hazard. Mater.* **2015**, 283, 657–662.
- (12) Mao, J.; Kim, S.; Wu, X. H.; Kwak, I.-S.; Zhou, T.; Yun, Y.-S. A Sustainable Cationic Chitosan/E. Coli Fiber Biosorbent for Pt(IV) Removal and Recovery in Batch and Column Systems. *Sep. Purif. Technol.* **2015**, *143*, 32–39.
- (13) Won, S. W.; Lim, A.; Yun, Y.-S. Recovery of High-Purity Metallic Pd from Pd(II)-Sorbed Biosorbents by Incineration. *Bioresour. Technol.* **2013**, *137*, 400–403.
- (14) Mpinga, C. N.; Bradshaw, S. M.; Akdogan, G.; Snyders, C. A.; Eksteen, J. J. The Extraction of Pt, Pd and Au from an Alkaline Cyanide Simulated Heap Leachate by Granular Activated Carbon. *Miner. Eng.* **2014**, *55*, 11–17.
- (15) Seyedhakimi, A.; Bastami, S. A.; Ghassa, S.; Razavi, H.; Chehreh Chelgani, S. Exploring Relationships between Various Activations of Granular Activated Carbon on Silver and Gold Adsorption: A Kinetic and Equilibrium Study. Sep. Sci. Technol. 2019, 54, 1710–1721.
- (16) An, F.-Q.; Li, M.; Wu, R.-Y.; Hu, T.-P.; Gao, J.-F.; Yuan, Z.-G. Effective Recovery of AuCl4— Using D301 Resin Functionalized with Ethylenediamine and Thiourea. *Hydrometallurgy* **2017**, *169*, 356—361.
- (17) Choudhary, B. C.; Paul, D.; Borse, A. U.; Garole, D. J. Surface Functionalized Biomass for Adsorption and Recovery of Gold from Electronic Scrap and Refinery Wastewater. *Sep. Purif. Technol.* **2018**, 195, 260–270
- (18) Wu, C.; Zhu, X.; Wang, Z.; Yang, J.; Li, Y.; Gu, J. Specific Recovery and In Situ Reduction of Precious Metals from Waste To Create MOF Composites with Immobilized Nanoclusters. *Ind. Eng. Chem. Res.* **2017**, *56*, 13975–13982.
- (19) Wang, C.; Liu, D.; Lin, W. Metal-Organic Frameworks as A Tunable Platform for Designing Functional Molecular Materials. *J. Am. Chem. Soc.* **2013**, *135*, 13222–13234.
- (20) Cheng, P.; Wang, C.; Kaneti, Y. V.; Eguchi, M.; Lin, J.; Yamauchi, Y.; Na, J. Practical MOF Nanoarchitectonics: New Strategies for Enhancing the Processability of MOFs for Practical Applications. *Langmuir* **2020**, *36*, 4231–4249.
- (21) O'Keeffe, M.; Yaghi, O. M. Deconstructing the Crystal Structures of Metal-Organic Frameworks and Related Materials into Their Underlying Nets. *Chem. Rev.* **2012**, *112*, 675–702.
- (22) Springthorpe, S. K.; Dundas, C. M.; Keitz, B. K. Microbial Reduction of Metal-Organic Frameworks Enables Synergistic Chromium Removal. *Nat. Commun.* **2019**, *10*, 5212.
- (23) Sun, D. T.; Gasilova, N.; Yang, S.; Oveisi, E.; Queen, W. L. Rapid, Selective Extraction of Trace Amounts of Gold from Complex Water Mixtures with a Metal—Organic Framework (MOF)/Polymer Composite. J. Am. Chem. Soc. 2018, 140, 16697—16703.
- (24) Palmer, R. H.; Liu, J.; Kung, C.-W.; Hod, I.; Farha, O. K.; Hupp, J. T. Electroactive Ferrocene at or near the Surface of Metal—Organic Framework UiO-66. *Langmuir* 2018, 34, 4707–4714.
- (25) Kanaizuka, K.; Sasaki, S.; Nakabayashi, T.; Masunaga, H.; Ogawa, H.; Hikima, T.; Takata, M.; Haga, M.-a. Observation of an Orientation Change in Highly Oriented Layer-by-Layer Films of a Ruthenium Complex upon Oxidation Reaction. *Langmuir* **2015**, *31*, 10327–10330.
- (26) Shi, L.; Dong, H.; Reguera, G.; Beyenal, H.; Lu, A.; Liu, J.; Yu, H.-Q.; Fredrickson, J. K. Extracellular Electron Transfer Mechanisms between Microorganisms and Minerals. *Nat. Rev. Microbiol.* **2016**, *14*, 651–662.
- (27) Hau, H. H.; Gralnick, J. A. Ecology and Biotechnology of the Genus Shewanella. *Annu. Rev. Microbiol.* **2007**, *61*, 237–258.
- (28) Tokunou, Y.; Okamoto, A. Geometrical Changes in the Hemes of Bacterial Surface c -Type Cytochromes Reveal Flexibility in Their Binding Affinity with Minerals. *Langmuir* **2019**, *35*, 7529–7537.
- (29) Burtch, N. C.; Jasuja, H.; Walton, K. S. Water Stability and Adsorption in Metal-Organic Frameworks. *Chem. Rev.* **2014**, *114*, 10575–10612.
- (30) Chevreau, H.; Permyakova, A.; Nouar, F.; Fabry, P.; Livage, C.; Ragon, F.; Garcia-Marquez, A.; Devic, T.; Steunou, N.; Serre, C.;

- Horcajada, P. Synthesis of the Biocompatible and Highly Stable MIL-127(Fe): From Large Scale Synthesis to Particle Size Control. *CrystEngComm* **2015**, *18*, 4094–4101.
- (31) Myers, C. R.; Nealson, K. H. Bacterial Manganese Reduction and Growth with Manganese Oxide as the Sole Electron Acceptor. *Science* **1988**, *240*, 1319–1321.
- (32) Rojas, S.; Baati, T.; Njim, L.; Manchego, L.; Neffati, F.; Abdeljelil, N.; Saguem, S.; Serre, C.; Najjar, M. F.; Zakhama, A.; Horcajada, P. Metal-Organic Frameworks as Efficient Oral Detoxifying Agents. J. Am. Chem. Soc. 2018, 140, 9581–9586.
- (33) Guesh, K.; Caiuby, C. A. D.; Mayoral, Á.; Díaz-García, M.; Díaz, I.; Sánchez-Sanchez, M. Sustainable Preparation of MIL-100(Fe) and Its Photocatalytic Behavior in the Degradation of Methyl Orange in Water. *Cryst. Growth Des.* **2017**, *17*, 1806–1813.
- (34) Sanchez-Sanchez, M.; de Asua, I.; Ruano, D.; Diaz, K. Direct Synthesis, Structural Features, and Enhanced Catalytic Activity of the Basolite F300-like Semiamorphous Fe-BTC Framework. *Cryst. Growth Des.* **2015**, *15*, 4498–4506.
- (35) Cornell, R. M.; Schwertmann, U. *The Iron Oxides*; Wiley-VCH Verlag GmbH & Co. KGaA, 2003.
- (36) Baron, D.; LaBelle, E.; Coursolle, D.; Gralnick, J. A.; Bond, D. R. Electrochemical Measurement of Electron Transfer Kinetics by Shewanella Oneidensis MR-1. *J. Biol. Chem.* **2009**, 284, 28865–28873.
- (37) Stookey, L. L. Ferrozine A New Spectrophotometric Reagent for Iron. *Anal. Chem.* **1970**, 42, 779–781.
- (38) Bradford, M. M. Rapid and Sensitive Method for the Quantitation of Microgram Quantities of Protein Utilizing the Principle of Protein-Dye Binding. *Anal. Biochem.* **1976**, 72, 248–254.
- (39) Xia, X.; Zhang, J.; Sawall, T. A Simple Colorimetric Method for the Quantification of Au(Iii) Ions and Its Use in Quantifying Au Nanoparticles. *Anal. Methods* **2015**, *7*, 3671–3675.
- (40) Liu, C.; Gorby, Y. A.; Zachara, J. M.; Fredrickson, J. K.; Brown, C. F. Reduction Kinetics of Fe(III), Co(III), U(VI), Cr(VI), and Tc(VII) in Cultures of Dissimilatory Metal-reducing Bacteria. *Biotechnol. Bioeng.* **2002**, *80*, 637–649.
- (41) Pongsajanukul, P.; Parasuk, V.; Fritzsche, S.; Assabumrungrat, S.; Wongsakulphasatch, S.; Bovornratanaraks, T.; Chokbunpiam, T. Theoretical Study of Carbon Dioxide Adsorption and Diffusion in MIL-127(Fe) Metal Organic Framework. *Chem. Phys.* **2017**, 491, 118–125.
- (42) Zhong, G.; Liu, D.; Zhang, J. Applications of Porous Metal—Organic Framework MIL-100(M) (M = Cr, Fe, Sc, Al, V). *Cryst. Growth Des.* **2018**, *18*, 7730–7744.
- (43) Simon, M. A.; Anggraeni, E.; Soetaredjo, F. E.; Santoso, S. P.; Irawaty, W.; Thanh, T. C.; Hartono, S. B.; Yuliana, M.; Ismadji, S. Hydrothermal Synthesize of HF-Free MIL-100(Fe) for Isoniazid-Drug Delivery. *Sci. Rep.* **2019**, *9*, 16907.
- (44) Kostka, J. E.; Dalton, D. D.; Skelton, H.; Dollhopf, S.; Stucki, J. W. Growth of Iron(III)-Reducing Bacteria on Clay Minerals as the Sole Electron Acceptor and Comparison of Growth Yields on a Variety of Oxidized Iron Forms. *Appl. Environ. Microbiol.* **2002**, *68*, 6256–6262.
- (45) Webster, J. G.; Mann, A. W. The Influence of Climate, Geomorphology and Primary Geology on the Supergene Migration of Gold and Silver. *J. Geochem. Explor.* **1984**, *22*, 21–42.
- (46) Mann, A. W. Mobility of Gold and Silver in Lateritic Weathering Profiles: Some Observations from Western Australia. *Econ. Geol.* **1984**, 79, 38–49.
- (47) Wu, C.; Zhu, X.; Wang, Z.; Yang, J.; Li, Y.; Gu, J. Specific Recovery and In Situ Reduction of Precious Metals from Waste To Create MOF Composites with Immobilized Nanoclusters. *Ind. Eng. Chem. Res.* **2017**, *56*, 13975–13982.
- (48) Huang, Z.; Zhao, M.; Wang, C.; Wang, S.; Dai, L.; Zhang, L.; Xu, L. Selective Removal Mechanism of the Novel Zr-Based Metal Organic Framework Adsorbents for Gold Ions from Aqueous Solutions. *Chem. Eng. J.* **2020**, 384, 123343.

- (49) Wang, C.; Lin, G.; Zhao, J.; Wang, S.; Zhang, L. Enhancing Au(III) Adsorption Capacity and Selectivity via Engineering MOF with Mercapto-1,3,4-Thiadiazole. *Chem. Eng. J.* **2020**, 388, 124221.
- (50) Yen, C.-H.; Lien, H.-L.; Chung, J.-S.; Yeh, H.-D. Adsorption of Precious Metals in Water by Dendrimer Modified Magnetic Nanoparticles. J. Hazard. Mater. 2017, 322, 215–222.
- (51) Newman, J. D. S.; Blanchard, G. J. Formation of Gold Nanoparticles Using Amine Reducing Agents. *Langmuir* **2006**, 22, 5882–5887.
- (52) Cai, P.-J.; Xiao, X.; He, Y.-R.; Li, W.-W.; Chu, J.; Wu, C.; He, M.-X.; Zhang, Z.; Sheng, G.-P.; Lam, M. H.-W.; Xu, F.; Yu, H.-Q. Anaerobic Biodecolorization Mechanism of Methyl Orange by Shewanella Oneidensis MR-1. *Appl. Microbiol. Biotechnol.* **2012**, *93*, 1769–1776.
- (53) Suresh, A. K.; Pelletier, D. A.; Wang, W.; Broich, M. L.; Moon, J.-W.; Gu, B.; Allison, D. P.; Joy, D. C.; Phelps, T. J.; Doktycz, M. J. Biofabrication of Discrete Spherical Gold Nanoparticles Using the Metal-Reducing Bacterium Shewanella Oneidensis. *Acta Biomater.* **2011**, *7*, 2148–2152.
- (54) Wu, R.; Cui, L.; Chen, L.; Wang, C.; Cao, C.; Sheng, G.; Yu, H.; Zhao, F. Effects of Bio-Au Nanoparticles on Electrochemical Activity of Shewanella Oneidensis Wild Type and Δ omcA/MtrC Mutant. Sci. Rep. **2013**, 3, 3307.
- (55) Swanner, E. D.; Maisch, M.; Wu, W.; Kappler, A. Oxic Fe(III) Reduction Could Have Generated Fe(II) in the Photic Zone of Precambrian Seawater. *Sci. Rep.* **2018**, *8*, 4238.
- (56) Long, J. R.; Yaghi, O. M. The Pervasive Chemistry of Metal—Organic Frameworks. *Chem. Soc. Rev.* **2009**, *38*, 1213–1214.
- (57) Yang, T.; Yu, D.; Wang, D.; Yang, T.; Li, Z.; Wu, M.; Petru, M.; Crittenden, J. Accelerating Fe(III)/Fe(II) Cycle via Fe(II) Substitution for Enhancing Fenton-like Performance of Fe-MOFs. *Appl. Catal., B* **2021**, *286*, 119859.